Supplementary Information for
Valproate Coenzyme-A Conjugate Blocks Opening of Receptor Binding Domains in the Spike Trimer of SARS-CoV-2 through an Allosteric Mechanism

Federica Maschietto[1,a], Tianyin Qiu[1,a], Jimin Wang[2,a,*], Yuanjun Shi[1], Brandon Allen[1], George P. Lisi[3], Elias Lolis[4], and Victor S. Batista[1,*,$]

[1]Department of Chemistry, Yale University, New Haven, CT 06520-8449, USA. [2]Department of Molecular Biophysics and Biochemistry, Yale University, New Haven, CT 06520-8114, USA.

[3]Department of Molecular and Cell Biology and Biochemistry, Brown University, Providence, RI 02912.

[4]Department of Pharmacology, Yale University, New Haven, CT 06520-8066.

[a]These authors made equal contributions to this study.

*Jimin Wang, Victor S. Batista
Email: jimin.wang@yale.edu, victor.batista@yale.edu

This PDF file includes:

Supplementary text
Figures S1 to S4

Supplementary Text

Motions of the RBD relative to S2 in the spike trimer

Figure S4A shows the rocking motion of individual RBD subunits relative to the equilibrated structure of the RBD trimer as a function of time along the MD trajectory for both VPA-CoA bound and apo structures, as prepared from pre-equilibrated state of the 3-fold symmetric 6vxx structure (23). We find that the equilibrated state corresponds to the energy minimum basin of the VPA-CoA bound complex. However, the apo structure transits to another local minimum (frames near 15 ns) before it finds the global minimum energy basin after 50 ns of dynamics (Figure S4). We find that the rmsF of Cα atoms are proportional to the magnitudes of RBD reorientations (Figure S4A, S4B) particularly when comparing the individual ligand-bound RBD relative to ligand-free RBD trimers.

The observed reorientation of the individual RBDs in the spike trimer involves a rotation of the RBDs relative to the trimeric S2 fragment. The pseudo-3-fold axis of the RBD trimer changes its orientation over time along the MD simulations relative to that of the trimer of S2 fragment. The apo structure shows a rotation of the RBD trimer close to 10° relative to the S2 trimer (Figure 7C), while in the VPA-CoA complex, the corresponding rotations vary along the trajectory exhibiting configurations that can be grouped into three clusters: (i) ~ 7° (< 50 ns), (ii) ~ 20° (> 90 ns), and (iii) ~ 32° (other time steps). The third group of configurations exhibits a rocking motion, responsible for degradation of the resolution of the MD-ESP maps. This rotation, however, is likely due to the absence of the neighboring N-terminal domains that surround the RBDs in the full-length spike protein.

Supplementary Figures

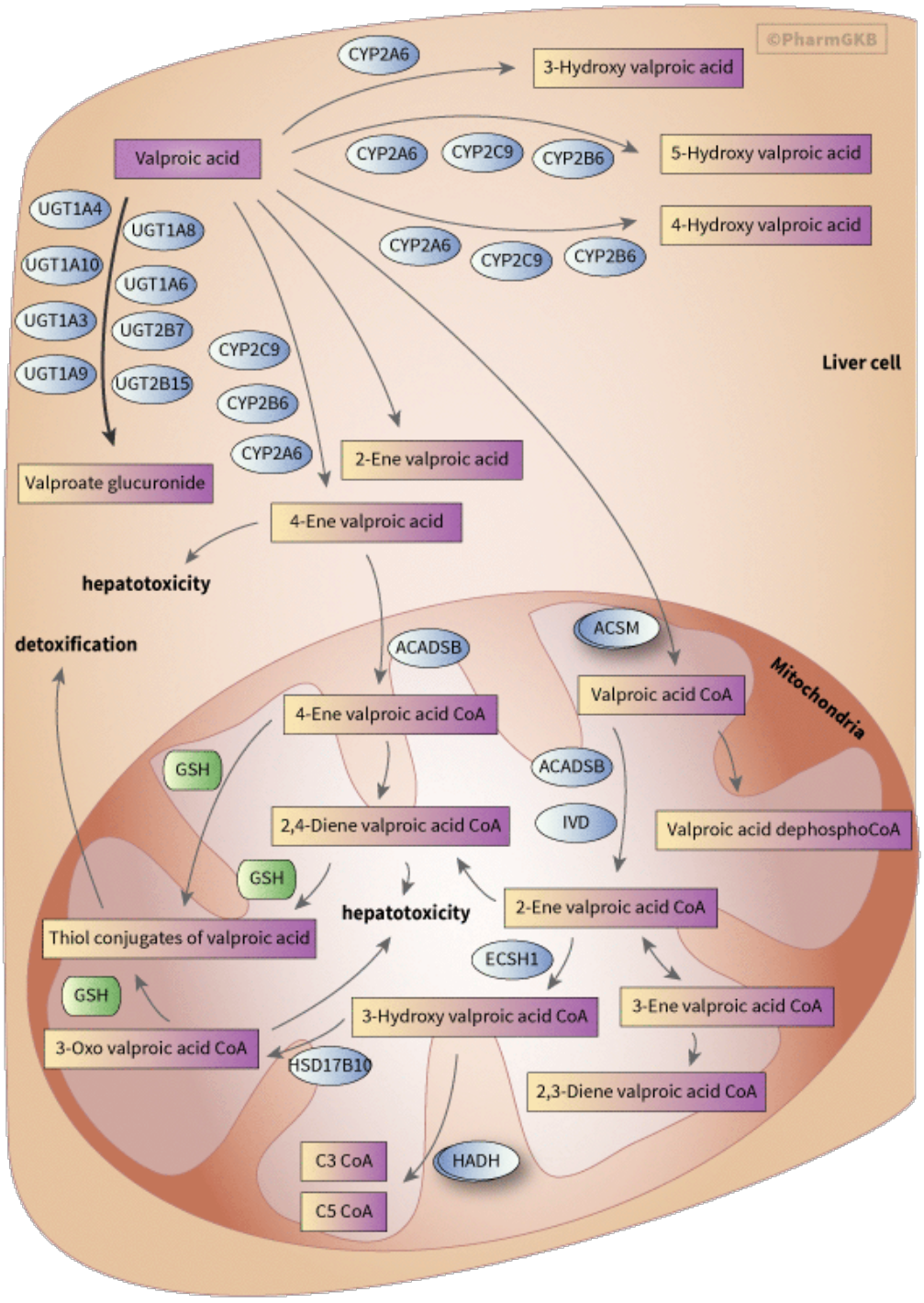

Fig. S1. Graphic representation of the metabolic intermediates involved in valproic acid pharmacokinetics. All intermediated were found to bind favorably in the pocked at the interface between the three RBD of the spike protein (with Docking Scores within the top 10% and displaying favorable interactions). MD simulations to validate the efficacy of other CoA variants and their stereoisomers (other than 3-oxo-valproic acid CoA used in this study). Graphics adapted from: https://www.pharmgkb.org/pathway/PA165964265.

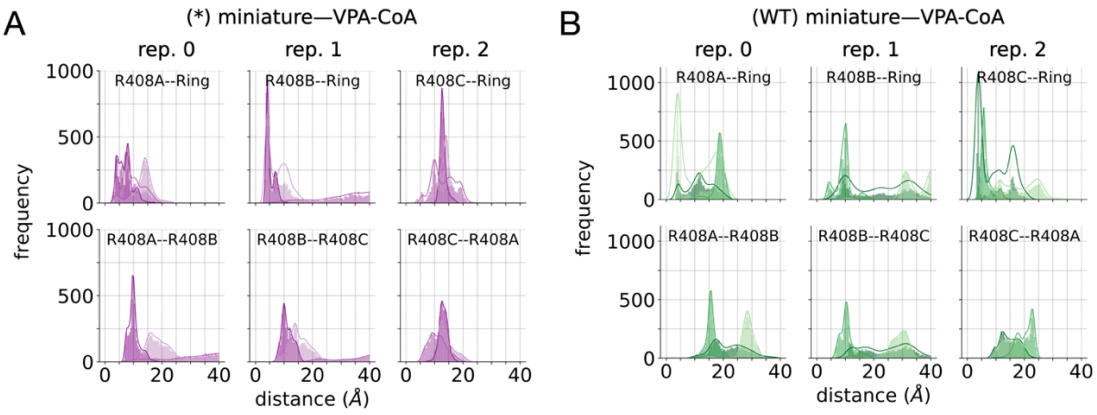

Fig. S2. Pore size across three different 400 ns replicas of simulations for the wild type (WT) and the K417N/L452R/D950N variant in complex with VPA-CoA. (A). Top row: distance distributions of R408(*X*)/CZ to the ring (defined as the center of mass of the adenine ring in VPA-CoA, with *X* corresponding to each RBD chain – A, B, or C) across three different replicas of the variant (labeled as *) in complex with VPA-CoA. Bottom row: R408-R408 sidechain distance (computed between the center of mass of each guanidinium group of R408 residues belonging to adjacent chains). (B). Top row: distance distributions of R408(*X*)/CZ to the ring. Bottom row: R408-R408 sidechain distance.

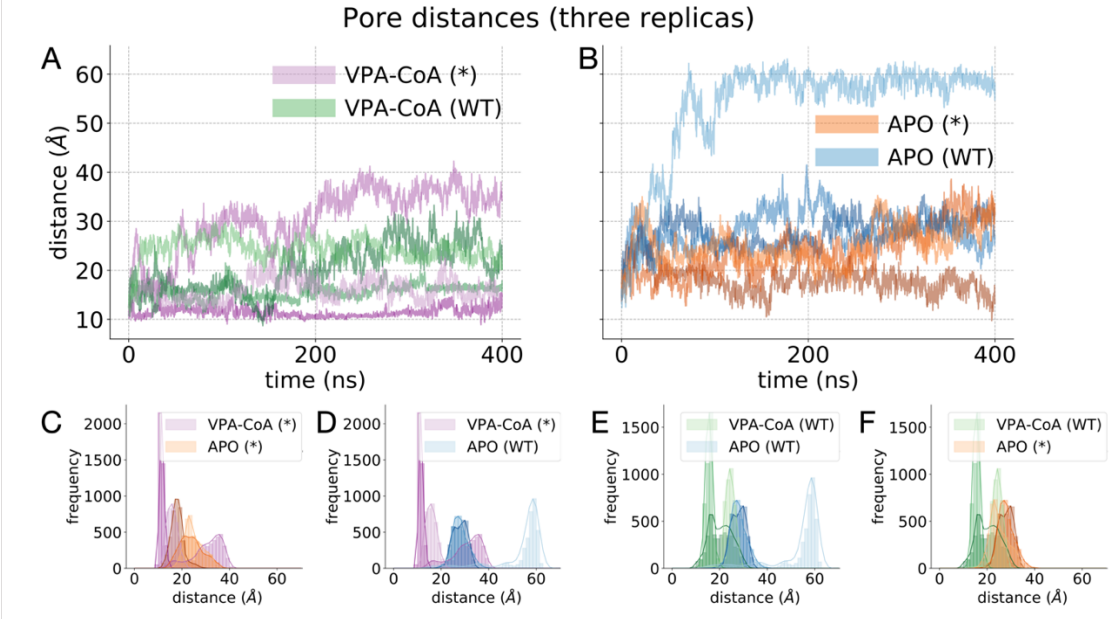

Fig. S3. Distribution of pore distances across three 400 ns replicas of simulations for WT and the K417N/L452R/D950N variant between the apo state and the VPA-CoA complex. (A) Distribution of R408-to-R408 distances on subunits A, B, or C across three different replicas of simulated MD of WT (purple palette) and the variant (green palette) spike construct in complex with VPA-CoA. (B) Distribution of average R408-to-R408 distances on subunits A, B, or C across three different replicas of simulated MD of the apo-WT (blue palette) and the variant (orange palette). Distance distributions corresponding to the R408-to-R408 curves in panels A and B are shown in panels C-F: (C) the apo state and the VPA-CoA complex of the variant, (D) the variant-VPA-CoA complex and the WT apo state,

(E) the WT apo state and the VPA-CoA complex, and (F) the apo variant and the WT VPA-CoA complex. Overall, VPA-CoA complexes show smaller pore distances relative to the apo state regardless of the WT or the variant.

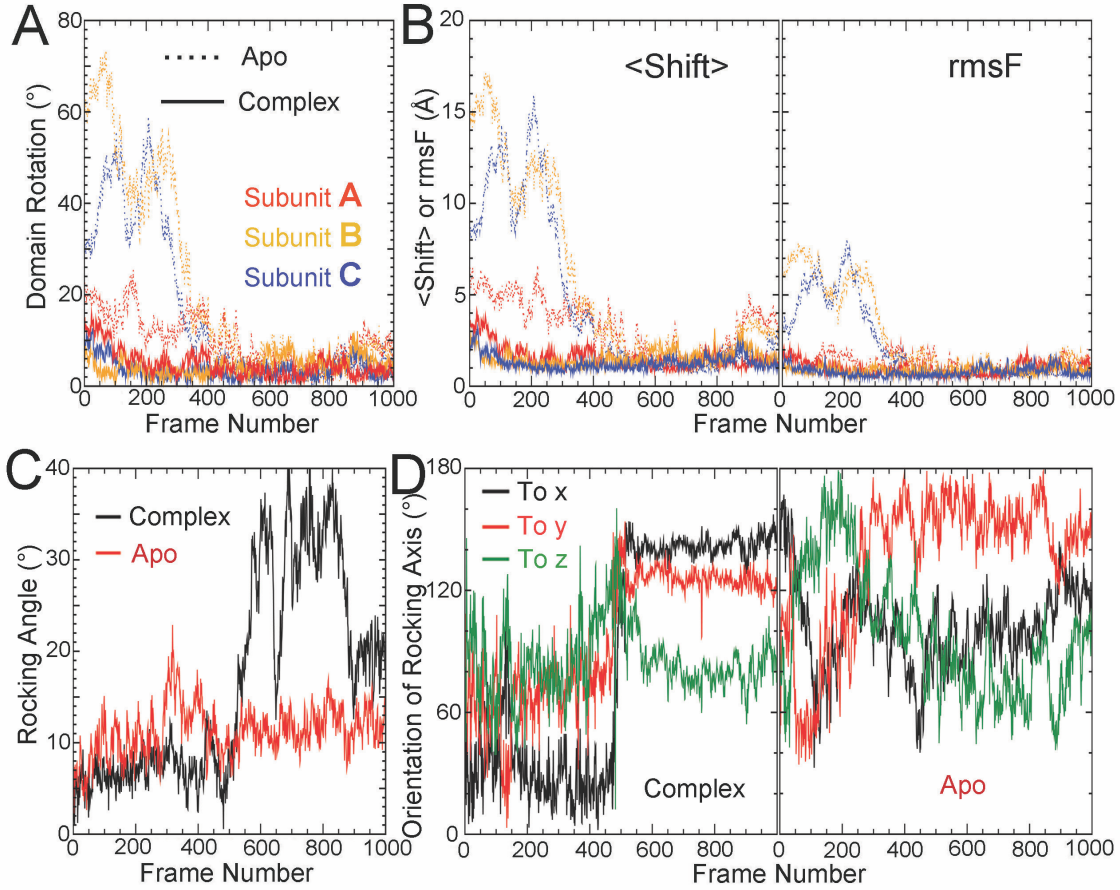

Figure S4. Domain rotations in MD trajectories as a function of frame. (A) Rotations of individual RBDs relative to the corresponding subunit of the equlibrated structure after three RBD were aligned for the VPA-CoA bound complex (solid) or the apo (dotted) structure. (B) Corresponding mean Cα shift to the equilibrated structure or Cα root-mean-squares fluctuation (rmsF). (C) Rotation of the three RBDs relative to the three S2 fragment for the VPA-CoA complex (black) and the apo (red) structures. (D) Orientations of domain rotation axis relative to three Cartesian axes (angle of the axis to *x*, black, *y*, red, and *z*, green) for the complex and apo structures.